American Journal of Pathology, Vol. 149, No. 2, August 1996

Clearance Kinetics, Biodistribution, and Organ Saturability of Phosphorothioate Oligodeoxynucleotides in Mice

Abdalla Rifai,* Wolfgang Brysch,† Kimberly Fadden,* Jeffrey Clark,‡ and Karl-Hermann Schlingensiepen§

From the Department of Pathology, Rhode Island Hospital, and Department of Medicine,‡ Roger Williams Hospital, Brown University School of Medicine, Providence, Rhode Island; Biognostik,† Göttingen, Germany; Laboratory for Molecular Tumor and Neurobiology,§ Max-Planck-Institute for Biophysical Chemistry, Göttingen, Germany*

We examined the dynamics of removal from circulation, tissue distribution, and persistence of phosphorothioate oligodeoxynucleotides (S-ODN) anti-tumor-necrosis-factor and a control of random sequence (randomer) in mice. After intravenous injection, the majority (96%) of S-ODN cleared rapidly from the circulation in the first two phases. In the first phase, 37.8 ± 2.3% of the radioactivity had a mean half-life ($t_{1/2}$) of 2.0 ± 0.4 minutes. In the second phase, 58.1 ± 1.5% of the radioactivity cleared with $t_{1/2}$ of 12.6 ± 0.2 minutes. The catabolic phase, constituting a minor proportion (4.1 ± 0.8% of the total radioactivity), had a mean $t_{1/2}$ of 2.7 ± 0.5 hours. At a low dose (1 μg) tissue distribution of both S-ODN anti-tumor-necrosis-factor and randomer were similar. The liver and kidneys were the major organs involved in uptake and removal of S-ODN. Autoradiographic studies showed the liver Kupffer cells to be the major site of uptake and renal urinary space for elimination. The clearance rate from the circulation was increased with the dose of S-ODN. In contrast, the fraction of radioactivity localized in the kidneys, liver, and spleen was decreased with increase in dosage. Furthermore, at a high dose (200 μg), the tissue distribution of the S-ODN anti-tumor-necrosis-factor differed significantly from the randomer. These findings have general significance in showing that the liver and kidneys are the major organs for removal of S-ODN and these organs are saturable at high doses. In addition, the results have specific importance in defining different parameters, dose and base composition, that affect utilization of antisense oligonucleotides for controlling gene expression* in vivo. *(Am J Pathol 1996, 149:717–725)

The pleiotropic cytokine tumor necrosis factor (TNF) is a primary mediator in the pathogenesis of infection and inflammation.[1] Tissue damage occurs as a consequence of TNF eliciting chemotactic cytokines, adhesion structures for leukocytes, prostaglandin synthesis, and platelet-activating factor production by endothelial cells. In addition, TNF evokes prothrombotic responses in endothelial cells with increases in tissue type plasminogen activator and decreases in the thrombomodulin-protein C anti-coagulation pathway. Because of its tissue destructive effect, TNF is generally considered to be an abnormal and deleterious response that plays a limited role in host defenses against bacterial and viral infection and thus has been considered a target for therapeutic intervention to ameliorate host toxic responses.

In our efforts to elucidate the inflammatory mediators involved in pathogenesis of IgA nephropathy,[2,3] we used synthetic oligodeoxynucleotides (ODNs) in an attempt to silence, at the transcription level, the expression of the proinflammatory TNF gene. Through base pairing, the antisense ODN binds to complementary mRNA and prevents the cell from producing a specific protein. Several studies have utilized antisense oligonucleotides to inhibit expression of a number of cellular and viral genes.[4,5] Phosphorothioate-modified oligodeoxynucleotides (S-ODNs), developed by Eckstein,[6] have several

Supported by National Institutes of Health grant DK49361.

Accepted for publication April 16, 1996.

Address reprint requests to Dr. Abdalla Rifai, Department of Pathology, Rhode Island Hospital, 593 Eddy Street, Providence, RI 02903.

properties required for effective antisense molecules *in vivo*. They specifically hybridize to target mRNA, are able to be taken up by cells, and are considerably more resistant against eukaryotic endonucleases and exonucleases than unmodified ODNs. This latter attribute of stability under biological conditions makes S-ODN antisense compounds ideal for a prolonged inhibition of cytokine gene expression.

Successful application of S-ODNs in pathophysiological and therapeutic studies, however, requires prior demonstration that there is significant S-ODN uptake by the target tissue. In addition, establishing the relationship between the dose of S-ODN, drug plasma concentration, tissue distribution and disposition allows for a rational approach to individualize and optimize antisense regimens for experimental *in vivo* studies. To achieve this objective, we have examined the clearance kinetics, tissue distribution, and persistence of S-ODN antisense to TNF-α and a control of random sequence in mice.

Materials and Methods

S-ODN Preparation

The S-ODNs were synthesized and purified as described previously.[7] Briefly, oligonucleotides were synthesized on an Applied Biosystems model 394 DNA synthesizer using β-cyanoethyl phosphoramidites and a 30-minute sulfurization step with 0.5 g of elemental sulfur, 4.8 ml of CS2, 4.8 ml of pyridine, and 0.4 ml of triethylamine. The S-ODN anti-TNF sequence (CAG AAG AGC GTG GT) is complementary to the sequence region 218 to 231 of human TNF-α[8] and the sequence region 276 to 289 of murine TNF-α.[9] The S-ODN random control (GTC CCT ATA CGA AC) is not complementary or homologous to any sequenced gene in the GenBank rodent database. Oligodeoxynucleotides were purified by reverse phase high performance liquid chromatography on a Waters Delta-Pak C18 column and detritylation with 80% acetic acid, extraction with diethyl ether, lyophilization, and dissolution in water. The S-ODNs were purified further by anion exchange chromatography on a Waters Protein-Pak DEAE 8HR column. The gradient was 10 to 100% B, linear over 45 minutes and held for 10 minutes. Buffer A contained 25 mmol/L Tris/Cl, 1 mmol/L EDTA, pH 8.0, 10% acetonitrile; buffer B contained 2.5 mol/L NaCl in buffer A. The S-ODN eluted around 90% B. The pooled eluates were mixed with two volumes of 100% ethanol to precipitate the S-ODNs, followed by dissolution in water and lyophilization.

Homogeneity concerning substitution of oxygen residues with thioate residues was analyzed as previously described[7] by ^{31}P nuclear magnetic resonance spectroscopy using a Bruker spectrometer at 162 MHz and 22°C.

Homogeneity with respect to length was analyzed by a P/ACE capillary electrophoresis system (Beckman Instruments) using an eCAP single-stranded DNA (ssDNA) 100 denaturing polyacrylamide capillary column and Tris-borate urea buffer. Samples at a concentration of 10 μg/ml were loaded into the sample vial. After the capillary column equilibration run, the sample was injected for 2 seconds, voltage 7.5 kV, and separated by constant voltage of 11.1 kV at 30°C and ultraviolet detection at 260 nm. Chromatogram data were managed by Gold System V 7.11 (Beckman Instruments).

Radioiodination of S-ODNs

The radiolabeling reaction of oligonucleotides was performed via a 5′ C6-amino linker (Glen Research, VA). The amino moiety was then radiolabeled using ^{125}I-labeled Bolton-Hunter reagent (Amersham, Arlington Heights, IL). Briefly, 200 μCi of ^{125}I-labeled Bolton-Hunter reagent was dried in a gentle stream of nitrogen. Oligonucleotides (50 μg), dissolved in 30 μl double-distilled dimethylformamide, were added to the air-dried reagent. After incubation on ice for 1 hour, 30 μl of borate-buffered saline (pH 8.0) was added to the tube. The reaction mixture tube was rotated overnight at 4°C. The reaction was stopped by adding 10 μl of 1 mol/L Tris buffer. Unbound radioiodine was removed by gel centrifugation over a Biospin 6 column (Bio-Rad, Richmond, CA). The S-ODNs were precipitated with ethanol/$MgCl_2$ followed by vacuum drying of the pellets. The specific activity of the radioiodinated S-ODNs was 3.3×10^5 to 1.1×10^6 cpm/μg and 1.4×10^5 to 4.2×10^5 cpm/μg for the anti-TNF and randomer, respectively.

Animal Experiments

Female, 2- to 3-month-old BALB/c mice were obtained from the Jackson Laboratory (Bar Harbor, ME). Radioiodinated S-ODNs in 0.2 ml of sterile saline were administered into the tail vein. From each experimental group of three mice, sequential blood samples (20 μl) were obtained from the retro-orbital venous plexus at 1, 2.5, 5, 10, 30, 60, 120, 240, and 360 minutes. The blood samples were expelled into 200 μl of 10 mmol/L EDTA to prevent any potential nuclease activity. Excess $MgCl_2$ was added to each

sample, followed by 0.6 ml of cold ethanol. Samples were kept on ice for 30 minutes and then centrifuged at 12,000 × *g* for 20 minutes. The supernatant and pellet of each sample were counted in a gamma counter.

The values of ethanol-precipitable radioactivity remaining in the blood were used to derive clearance curves; the first three data points were used to extrapolate the zero time value by linear regression analysis. The means and standard deviations were calculated for each time point, plotted, and analyzed by linear regression analysis.[10] The elimination rate constant (*Kel*) was derived from the slope of the curve (slope = *Kel*/2.303), which was calculated by linear regression analysis. The half-life ($t_{1/2}$) of circulating S-ODNs was determined from the expression, $t_{1/2} = 0.693/Kel$.

Organ distribution of the S-ODNs was determined at 10, 60, and 360 minutes when monitoring of the removal of radioactivity from the circulation of each experimental group (three mice/group) was terminated. The mice were anesthetized with pentobarbital followed immediately by incision of the thoracic cavity. The heart, kidneys, liver, and lungs were rendered free of blood by perfusion of 10 ml of saline through the left ventricle. Correction for the intravascular blood content of the remaining organs was based on established values for volume of blood in mouse tissue[11]: carcass (45 μl/g tissue), gastrointestinal tract (48 μl/g tissue), skin (30 μl/g tissue), and spleen (179 μl/g tissue). All of the excised organs and tissues were weighed before measurement of radioactivity. The amount of radioactivity within each organ was counted in an LKB gamma scintillator and the values were expressed as a percentage of the total amount administered or as a percentage of dose per gram of tissue.

The data for clearance kinetics and organ uptake were evaluated for statistical significance by the *t*-test or analysis of variance, using SigmaStat (Jandel Scientific, San Rafael, CA).

Autoradiography

The ^{125}I-radiolabeled S-ODN anti-TNF, 6 μCi (5.3 μg) in saline, was administered intravenously. Mice were anesthetized at 10 or 60 minutes after the injection and organs rendered blood-free by left ventricle perfusion of saline. Kidney and liver slices were fixed overnight with buffered 10% formalin. Paraffin-embedded tissue sections on poly-L-lysine-treated slides were cleared of paraffin before coating with NTB-3 nuclear tract emulsion (Eastman Kodak, Rochester, NY). The emulsion-coated slides were exposed for 5 to 12 days at 4°C. The emulsion was then developed with D19 (Kodak) and fixed with 20% sodium thiosulfate. The slides were stained with hematoxylin and eosin (H&E).

For electron microscope autoradiography, a dose containing 12 μCi (10.6 μg) of S-ODN anti-TNF was administered into the tail vein of a mouse that was anesthetized at 10 minutes after injection. Liver perfusion, *in situ* fixation, and preparation of tissue sections for electron microscope autoradiography were described previously.[12] The tissue section grids, placed on slides, were coated with formvar followed by Ilford nuclear emulsion L4 (Polysciences, Warrington, PA) as described by Kornhauser et al.[13] Emulsion-coated sections were exposed at 4°C for 6 to 12 weeks and developed with D19 (Kodak). The preparations were examined with a Philips 500 electron microscope.

Results

Characterization of S-ODN

A tandem of purification procedures consisting of reverse-phase high performance liquid chromatography and anion exchange chromatography made it possible to prepare uniform S-ODN oligomers. Sulfurization of the phosphor linkages was virtually complete as determined by ^{31}P nuclear magnetic resonance spectroscopy (data not shown). Homogeneity of the S-ODN preparations was evaluated by capillary gel electrophoresis. The 14-mer S-ODN anti-TNF showed 99.7% purity (Figure 1A). The S-ODN random sequence showed 87.6% purity (Figure 1B) with two additional shorter oligomer peaks accounting for 9.5 and 2.9% of the S-ODN.

Blood Clearance of TNF Antisense

The initial experiments were designed to determine the kinetics of S-ODN anti-TNF in the circulation of mice. An intravenous bolus dose (1 μg) of radioiodinated S-ODN anti-TNF was used to measure the disappearance of radioactivity from the circulation during a 6-hour period. At the end of this period, less than 1% of the injected radioactive S-ODN was detectable in the circulation. The disappearance curve consisted of three exponential components, determined by graphic resolution in conjunction with linear regression analysis (Figure 2). The initial fast component lasted for 8.6 ± 1.8 minutes and had a mean half-life ($t_{1/2}$) of 2.0 ± 0.4 minutes with 37.8 ± 2.3% of the radioactivity removed from the circula-

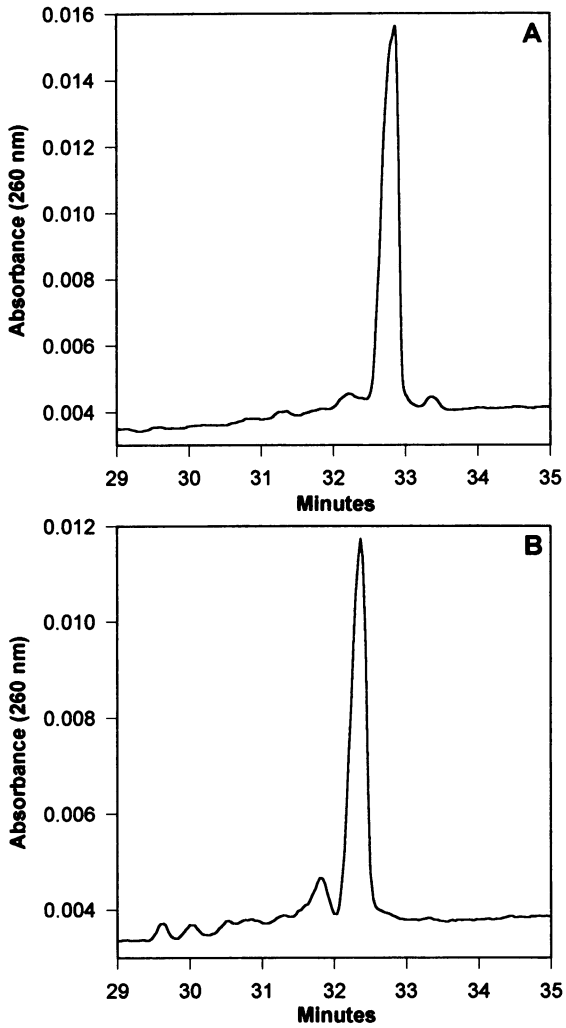

Figure 1. *Chromatographic profile of purified S-ODN anti-TNF* (A) *and random 14-mer* (B) *obtained by capillary polyacrylamide gel electrophoresis. Samples (10 μg/ml) were injected electrokinetically for 2 seconds at 7.5 kV and separated for 60 minutes at 11 kV on eCAP ssDNA column.*

tion with this half-life. The second component lasted approximately 1 hour and had a mean $t_{1/2}$ of 12.6 ± 0.2 minutes and 58.1 ± 1.5% of the radioactivity cleared from circulation with this half-life. The third component, which represented the catabolic phase, constituted 4.1 ± 0.8% of the total radioactivity and had $t_{1/2}$ of 2.7 ± 0.5 hours. Based on such $t_{1/2}$ values, this phase may last between 12 and 18 hours.

The fraction of nonprecipitable radioactivity in each blood sample amounted to less than 1% of the zero-timed blood sample. Furthermore, there was no discernible or significant increase in the nonprecipitable radioactivity during the 6-hour period of clearance to indicate S-ODN degradation.

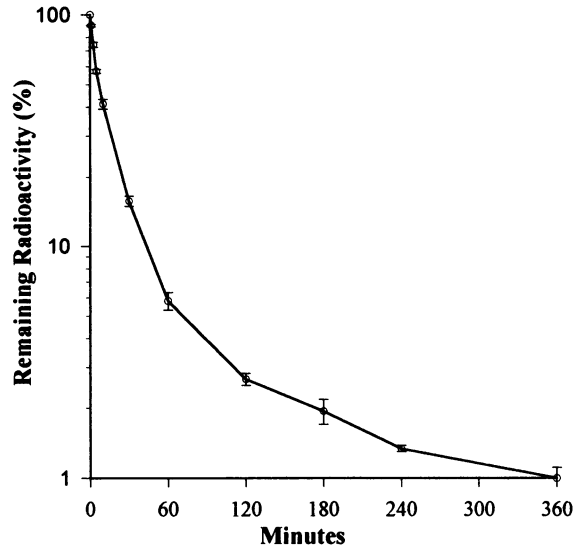

Figure 2. *Clearance of S-ODN anti-TNF from the circulation of mice. Each data point represents the mean ± 1 SD of radioactivity in blood samples obtained sequentially from three mice.*

TNF Antisense Tissue Distribution

To assess the fate of circulating S-ODN anti-TNF, the organ and tissue distribution of the TNF antisense was examined 10, 60, and 360 minutes after intravenous injection. In the first 10 minutes, most of the antisense removed from circulation localized in the liver and kidneys (Table 1). During this period, a significant amount of the S-ODN anti-TNF also localized in two other large organs, the gastrointestinal tract and skin. Unlike the liver and kidneys, however, the radioactivity in these two large organs increased at 60 minutes. Disappearance of the S-ODN anti-TNF from the renal and hepatic tissues was a concomitant process with its uptake as evidenced by the maximal amount of radioactivity at 10 minutes and significant decline at 1 hour. In general, persistence of the S-ODN anti-TNF in the different tissues was relatively short ($t_{1/2}$ = 2.7 ± 0.6 hours). The total

Table 1. *Distribution and Persistence of S-ODN Anti-TNF (1 μg) in Tissues at Timed Intervals after Injection*

Tissue	10 minutes	60 minutes	360 minutes
Carcass	9.70 ± 1.33	9.62 ± 1.63	3.51 ± 0.09
Gastrointestinal tract	8.12 ± 1.18	12.64 ± 0.79	4.49 ± 0.69
Heart	0.27 ± 0.02	0.17 ± 0.02	0.04 ± 0.01
Kidneys	19.49 ± 0.01	14.72 ± 0.15	2.91 ± 0.31
Liver	24.69 ± 2.45	16.06 ± 0.38	5.34 ± 0.40
Lungs	0.52 ± 0.11	0.45 ± 0.13	0.18 ± 0.03
Skin	6.83 ± 1.79	9.06 ± 1.42	2.70 ± 0.26
Spleen	0.89 ± 0.19	0.73 ± 0.02	0.18 ± 0.01

Data represent the mean ± 1 SD percent value of administered radioactivity into groups of three mice.

amount of radioactivity detectable in the tissues declined from 78% of the total administered dose at 10 minutes to 19.8% after 360 minutes. Regression analysis of the sum of detectable radioactivity in the different tissues and organs at 10, 60, and 360 minutes showed a total body elimination rate of approximately 2.9 hours. Measurement of the radioactivity in the thyroid gland failed to show any significant increase between 10 and 360 minutes.

Hepatic and Renal Localization of TNF Antisense

To determine the mechanism of S-ODN anti-TNF removal from the circulation, light and electron microscope autoradiography was performed to identify the site of localization in liver and kidneys. To avoid the potential of cell-to-cell radioactivity transfer usually associated with breakdown products, autoradiography was performed on hepatic and renal specimens obtained 10 minutes after administration of radioiodinated antisense. The distribution of the autoradiographic grains in the kidneys was predominant in the glomerular urinary space and lumen of the proximal and distal tubules (Figure 3a). By electron microscope autoradiography, only few silver grains could be detected without being cellular specific.

The majority of the detected autoradiographic grains in the liver were localized in the sinusoidal cells (Figure 3b). There was little or no autoradiographic grains in the hepatocytes in the early removal phase. Electron microscope autoradiography revealed the Kupffer cells (Figure 3c) to be the major site that mediates hepatic uptake of S-ODNs. The silver grains were confined to cell surface processes and lysosomal structures. Examination of several ultrathin sections revealed no significant nuclear localization. Collectively, these results are suggestive of Kupffer cell uptake in the liver and passive transient filtration in the kidneys.

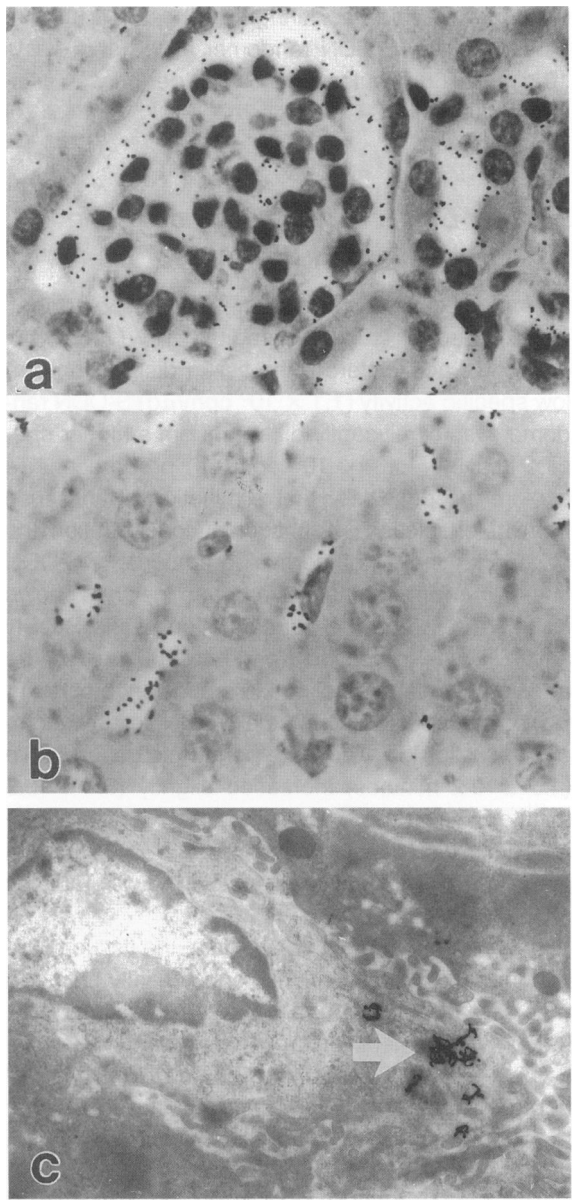

Figure 3. *Representative light and electron microscope autoradiographs of radioiodinated S-ODN anti-TNF in the kidneys and liver 10 minutes after injection.* **a:** *Cortical kidney section exhibiting the majority of radioactivity associated with urinary space in the glomerulus and tubules.* **b:** *Liver section showing concentrated localization of the radioactivity in the hepatic sinusoids. H&E; magnification, ×1000.* **c:** *Ultrastructural autoradiography of a liver section showing Kupffer cell with multiple silver grains* (**arrow**) *associated with lysosomal structures. Final magnification, ×10,920.*

Effect of S-ODN Composition on Clearance and Tissue Distribution

To determine whether the clearance of S-ODN anti-TNF represents a general phenomenon, we examined clearance kinetics and tissue distribution of a similarly sized (14-mer) S-ODN with random sequence (randomer). The overall 6-hour disappearance of the S-ODN randomer from the circulation showed three phases. Radioactivity in the initial phase, which accounted for 36.3 ± 3.1% of the administered dose, was rapidly eliminated ($t_{1/2}$ = 1.8 ± 0.2 minutes). The intermediate phase composition (57.1 ± 1.5%) was similar to that of S-ODN anti-TNF. However, the clearance rate during this phase ($t_{1/2}$ = 17.8 ± 0.7 minutes) was significantly ($P < 0.003$) slower than the TNF S-ODN. Although the composition of the slow phase was slightly more (7.7 ± 1.9%) than the S-ODN anti-TNF, the elimination rate (2.4 ±

0.4 hours) was similar during this phase. Tissue distribution of the S-ODN randomer at the end of the 10-minute, 60-minutes, and 6-hour period was similar overall to the S-ODN anti-TNF.

Effect of Dose on Blood Elimination and Tissue Distribution of Antisense

During the course of our studies we observed that, when an equal amount of radioactivity (1.1×10^6 cpm) was administered, the tissue distribution of a low specific activity (1.1×10^5 cpm/μg) S-ODN randomer was significantly different from a higher specific activity (1.13×10^6 cpm/μg) preparation. To explore the possibility that elimination of antisense from the circulation is a function of concentration, the clearance kinetics of increasing amounts of S-ODN anti-TNF and randomer were determined. As shown in Figure 4, when the concentration of the S-ODN anti-TNF was increased from 1 to 200 μg, by the addition of unlabeled oligos to a constant amount (1 μg) of ^{125}I-labeled S-ODN, the S-ODN anti-TNF composite $t_{1/2}$ for the 10-minute period clearance curve (4.5 ± 0.2 minutes) increased slightly (5.5 ± 0.5 minutes; $P = 0.0350$). By comparison, the $t_{1/2}$ of the randomer increased significantly ($P = 0.0110$) from 4.7 ± 0.7 minutes (1 μg dose) to 6.9 ± 0.4 minutes (200-μg dose).

In contrast to the clearance data, the tissue distribution of the S-ODN anti-TNF substantially changed with increasing dosage of S-ODN. A significant ($P < 0.0001$) decrement in the fraction of administered S-ODN anti-TNF deposition occurred in renal and hepatic tissues (Figure 5). These results suggest that the liver and kidneys are capacity-limited organs in the uptake of S-ODN.

The general phenomenon of the saturating effect of S-ODN dose on tissue distribution is highlighted by the similar results in the paired comparison of a low (1 μg) and a high (200 μg) dose S-ODN anti-TNF and randomer (Table 2). The decrement in liver, renal, and splenic uptake is accompanied by increased uptake in heart and skin. Other tissues, however, such as the gastrointestinal tract and lungs, are not affected by dose. At a low dose (1 μg) the tissue distribution of S-ODN anti-TNF was similar to S-ODN randomer. In contrast, at a high dose (200 μg), there was a lower uptake of randomer than S-ODN anti-TNF uptake in the deep tissue ($P = 0.0032$), heart ($P = 0.0070$), liver ($P = 0.0112$), and skin ($P = 0.0118$). These findings suggest a combinatorial effect of base composition and dose on S-ODN tissue localization.

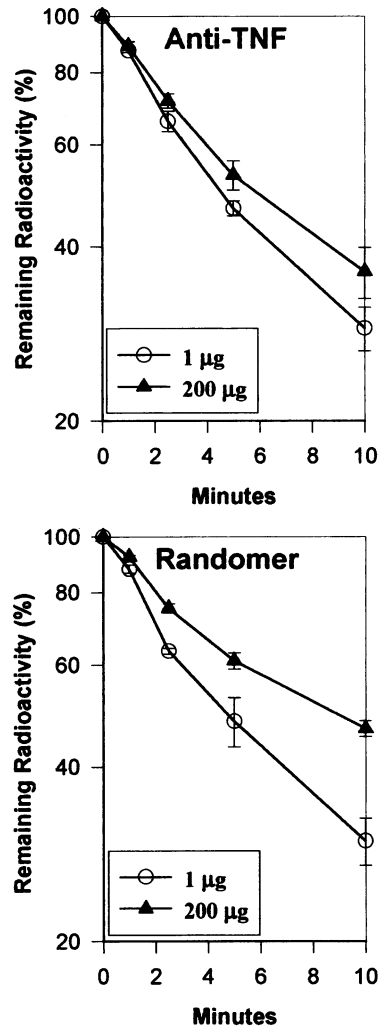

Figure 4. *The effect of dose on the clearance kinetics of S-ODN during the initial rapid phase of elimination.* Upper panel *demonstrates the slower elimination rate* ($t_{1/2} = 5.5 \pm 0.5$ *minutes) of 200* μg *than 1* μg ($t_{1/2} = 4.5 \pm 0.2$ *minutes) of* ^{125}*I-labeled S-ODN anti-TNF.* Lower panel *demonstrates similar effect of dose on clearance of randomer, 200* μg ($t_{1/2} = 6.9 \pm 0.4$ *minutes) and 1* μg ($t_{1/2} = 4.7 \pm 0.7$ *minutes). Each point represents the observed mean value ± 1 SD of three mice in each experiment.*

Discussion

In an attempt to extend studies showing that synthetic antisense oligonucleotides can be used to regulate TNF-α gene expression *in vitro*[14] to an *in vivo* setting, we evaluated their clearance kinetics, tissue distribution, and fate in mice. Radioiodinated TNF antisense and a control with random sequence allowed a paired comparison of the kinetics and fate of these phosphorothioate oligonucleotides. The presented data demonstrate that several parameters simultaneously play critical roles in the removal and ultimate fate of the oligonucleotides in tissues.

Clearance studies (Figure 2) indicate S-ODNs have a relatively short half-life in the circulation. A

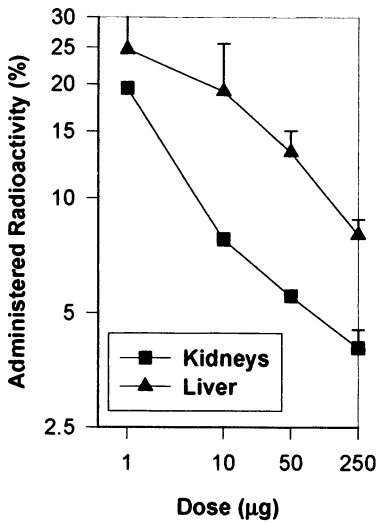

Figure 5. *Effect of dose on hepatic and renal uptake of ^{125}I-labeled S-ODN anti-TNF at 10 minutes after injection. Each data point represents the mean ± 1 SD for a group of three mice. The significance in decline was determined by analysis of variance, single factor, with a P value of 3.2×10^{-5} and 2.7×10^{-10} for the liver and kidneys, respectively.*

substantial portion (38%) of either S-ODN anti-TNF or randomer was removed at a relatively rapid rate ($t_{1/2}$ = 2 minutes). This is consistent with previous findings showing that ssDNA is rapidly eliminated from the circulation.[15] In those studies, hepatic uptake accounted for 90% of the large-sized ssDNA removal within 5 minutes of administration. However, S-ODN removal mechanisms may differ from those for large ssDNA. The lower hepatic uptake (25%) observed with S-ODN could be due to a size difference. Thus, whereas most of the large-sized ssDNA would be limited to the intravascular compartment and available for hepatic removal, the small-sized (14-mer) S-ODN diffuses more rapidly into the extravascular tissues or is removed in the kidneys (20%). This is consistent with the substantial amount (58%) of radioactivity that constitutes the intermediate phase of clearance reflecting equilibration between tissue and circulation. In a relatively short period (1 hour), the first two phases of tissue binding and distribution accounted for the removal of the major fraction (95%) of the S-ODNs from the circulation.

Previous studies utilizing high doses of ^{35}S- or ^{32}P-labeled S-ODNs, described tissue distribution of viral antisense in mice.[16,17] The kidneys were the major organ of uptake when ^{35}S-labeled human immunodeficiency virus tat antisense was utilized, whereas uptake in the liver was equivalent to that in lungs, spleen, and heart.[16] The decreased amount present in the liver may have been due to dose or to the unusual feature of chain length extension of the oligos in different organs. The prolonged persistence of the ^{35}S-labeled human immunodeficiency virus tat antisense in mouse tissue is also at variance with our results. Similar to our findings, the liver and kidneys were the major target organs in a study using ^{32}P-labeled oligos.[17] In contrast to our findings, however, the peak amount detected in this study at 10 minutes was less than 2% of the total injected radioactivity. Our experience in using ^{32}P-5′-end-radiolabeled S-ODN for *in vivo* studies was highly unsatisfactory because of their rapid (within 5 minutes) degradation by ubiquitous phosphatases.

Our findings also contrast with a recent report by Plenat et al[18] that described the cell and tissue distribution of 3′- and 5′-end-modified phosphodiester ODN in normal and tumor-bearing mice. Although modification of phosphodiester oligonucleotides at the 3′ end may offer protection against serum 3′-exonucleases (reviewed in Ref. 4), it is well established that despite modification of the 3′ and 5′ ends of phosphodiester ODN they are rapidly degraded by cellular endonucleases.[19,20] Furthermore, Fisher et al[20] demonstrated that fluorescent ODN metabolites, derived from the 5′ end modified with fluorescein and a 3′-end-protected phosphodiester ODN, undergo rapid cellular exocytosis. Accordingly, the fluorescent microscopy and immunohistological

Table 2. *Effect of Dose on the Tissue Distribution of S-ODN Anti-TNF and Randomer*

Tissue	Anti-TNF			Randomer		
	1 μg	200 μg	*P* value	1 μg	200 μg	*P* value
Carcass	0.4 ± 0.2	0.9 ± 0.2	0.0222	0.2 ± 0.1	0.2 ± 0.1	NS
Gastrointestinal tract	2.8 ± 0.6	2.8 ± 0.0	NS	3.0 ± 0.4	2.8 ± 0.5	NS
Heart	1.7 ± 0.4	3.8 ± 0.7	0.0105	1.5 ± 0.1	2.5 ± 0.3	0.0044
Kidneys	61.4 ± 6.4	12.8 ± 0.6	0.0002	68.1 ± 6.6	12.8 ± 1.7	0.0002
Liver	20.3 ± 2.9	7.2 ± 0.3	0.0015	22.7 ± 0.9	6.1 ± 0.2	0.0001
Lungs	2.2 ± 0.6	3.1 ± 0.5	NS	1.8 ± 0.2	2.6 ± 0.8	NS
Skin	2.1 ± 0.4	4.5 ± 0.9	0.0112	1.1 ± 0.3	2.2 ± 0.2	0.0065
Spleen	8.1 ± 1.1	4.2 ± 1.0	0.0119	5.5 ± 0.1	3.3 ± 0.4	0.0011

Data represent percent of administered dose per gram of tissue at 10 minutes after injection. Each value is the mean ± SD for a group of three mice. Statistical significance (*P* value) was analyzed by *t*-test. NS, not significant.

findings of Plenat et al[17] potentially may reflect tissue redistribution of fluorescein- or digoxigenin-conjugated metabolites of the degraded phosphodiester ODN.

Determination of the percent administered dose per gram of tissue (Table 2) indicated that the largest portion (>85%) of the S-ODN is processed by the liver and kidneys. This quantity was 25-fold the amount localized in the gastrointestinal tract and 40- to 50-fold higher than that of heart, lungs, skin, and carcass (muscle and bone). To determine the cellular site of the S-ODN uptake in liver and kidneys, light and electron microscopic autoradiography (Figure 3) was performed at 10 minutes, before the potential generation of significant degradation products. In the kidneys, most radioactivity was in the glomerular urinary space and tubular lumen. The S-ODNs in the liver localized predominantly in sinusoidal cells (Figure 3b). High resolution autoradiography (Figure 3c) revealed the Kupffer cells to be the major site of uptake. The 1-hour autoradiograms from the liver and kidneys (not shown) contained a decreased number of total silver grains but a similar distribution pattern to that observed at 10 minutes. These findings suggest that Kupffer cell uptake may represent an active process of elimination whereas the S-ODN localization in the kidneys reflects transient passage or filtration of the low molecular weight oligomers. Paucity of the S-ODNs in hepatocytes suggests cellular selectivity within an organ for binding or uptake of S-ODNs. The site of S-ODN localization in gastrointestinal tract and skin is unknown. The failure of 200 μg of S-ODN (Table 2) to saturate these tissues may indicate extracellular binding or slow diffusion of S-ODNs in these organs.

The rapid (average $t_{1/2}$ = 2.7 hr) disappearance of S-ODNs (Table 1) from tissues was surprisingly similar for all examined organs. If hepatic sinusoidal uptake of S-ODNs resulted in rapid degradation in nuclease-rich lysosomal compartments of Kupffer cells, then the expected rate of disappearance from the liver would be faster than in other organs. The cellular mechanisms involved in catabolism or exocytosis of S-ODNs are unknown. Organ uptake and catabolism may recapitulate the processes of S-ODN cellular binding, endocytosis, and exocytosis observed in *in vitro* studies.[5,21,22] The later process of cellular reflux may explain the similarity of S-ODN disappearance rate observed in different organs. The lack of increase in free ^{125}I radioactivity in blood or enhanced uptake by thyroid gland supports intact S-ODN exocytosis rather than catabolism.[5,21] An alternative possibility is that the S-ODN was retained in the extracellular compartment of the tissues. This also may explain the similarity of S-ODN elimination rate from plasma during the slow phase (2.7 hours), disappearance rate from different tissues (2.7 hours), and total body elimination rate (2.9 hours). Furthermore, gel electrophoresis of S-ODNs (data not shown) in urine collected during the 6-hour experiments indicated that more than 60% of the S-ODNs were intact. The organ and source of the degraded S-ODNs in urine have not been determined.

Although there are many similarities in the overall pharmacokinetics and distribution of different S-ODNs, the base composition of the S-ODNs may affect specific features of tissue distribution and clearance. We examined the potential influence of S-ODN base composition on clearance kinetics and tissue distribution by comparing the TNF antisense with a random sequence with lower purine content (TNF antisense, 73%; randomer, 43%). At a low dose of 1 μg (Table 2), both S-ODNs exhibited similar hepatic uptake, renal localization, and clearance patterns (Figure 4). In contrast, at a high dose (200 μg), the control randomer cleared significantly at a slower rate and distributed differently from the TNF antisense. The cause of this combinatorial effect of dose and base composition on S-ODN tissue distribution is unknown.

In conclusion, our results suggest that several parameters may affect the outcome of studies evaluating S-ODN antisense oligos to control gene expression *in vivo*. Rapid elimination of antisense from the circulation and uptake in liver Kupffer cells suggests the need to develop modification to S-ODNs to enhance their tissue localization and achieve cell targeting *in vivo*. Glomerular filtration contributes greatly to the rapid loss of S-ODN, and modulating this elimination process may enhance the usefulness of oligos. Saturation of tissue and organs with S-ODNs is affected by the limited processing capacity of the liver and kidneys. The dose and base composition of the S-ODNs also affect tissue distribution and persistence. Collectively, these results provide insights into modifications needed for successful utilization of antisense ODN to inhibit gene expression *in vivo*.

Acknowledgments

We thank Mr. Patrick Verdier, Rhode Island Hospital central research laboratory, for his valuable assistance in electron microscope autoradiography.

References

1. Tracey KJ, Cerami A: Tumor necrosis factor: a pleiotropic cytokine and therapeutic target. Annu Rev Med 1994, 45:491–503
2. Emancipator SN, Lamm ME: IgA nephropathy: pathogenesis of most common form of glomerulonephritis. Lab Invest 1989, 60:168–183
3. Rifai A: Immunopathogenesis of experimental IgA nephropathy. Springer Semin Immunopathol 1994, 16: 81–95
4. Uhlmann E, Peyman A: Antisense oligonucleotides: a new therapeutic principle. Chem Rev 1990, 90:543–584
5. Stein CA, Cheng YC: Antisense oligonucleotides as therapeutic agents: is the bullet really magical? Science 1993, 261:1004–1012
6. Eckstein F: Nucleoside phosphorothioates. Annu Rev Biochem 1985, 54:367–402
7. Brysch W, Rifai A, Tischmeyer W, Schlingensiepen K-H: Rational drug design, pharmacokinetics and organ uptake of antisense phosphorothioate oligodeoxynucleotides *in vivo*. Antisense Oligonucleotide therapy: Current Status. Edited by S Agrawal. New Jersey, Humana Press, 1994
8. Wang AM, Creasey AA, Ladner MB, Lin LS, Strickler J, Van Arsdell JN, Yamamoto R, Mark DF: Molecular cloning of the complementary DNA for human tumor necrosis factor. Science 1985, 228:149–154
9. Pennica D, Hayflick JS, Bringman TS, Palladino MA, Goeddel DV: Cloning and expression in *Escherichia coli* of the cDNA for murine tumor necrosis factor. Proc Natl Acad Sci USA 1985, 82:6060–6064
10. Rifai A, Mannik M: Clearance kinetics and fate of mouse IgA immune complexes prepared with monomeric or dimeric IgA. J Immunol 1983, 130:1826–1832
11. Altman PL, Dittmer DS: Volume of blood in tissue: vertebrates. Respiration and Circulation. Edited by PL Altman, DS Dittmer. Maryland, FASEB, 1971, pp 384
12. Emlen W, Rifai A, Magilavy D, Mannik M: Hepatic binding of DNA is mediated by a receptor on nonparenchymal cells. Am J Pathol 1988, 133:54–60
13. Kornhauser GV, Krum JM, Rosenstein JM: An innovative coating technique for light and electron microscopic autoradiography. J Histochem Cytochem 1992, 40:879–882
14. Witsell AL, Schook LB: Tumor necrosis factor-α is an autocrine growth regulator during macrophage differentiation. Proc Natl Acad Sci USA 1992, 89:4754–4758 (published erratum in Proc Natl Acad Sci USA 1993, 90:4763)
15. Emlen W, Mannik M: Kinetics and mechanisms for removal of circulating single-stranded DNA in mice. J Exp Med 1978, 147:684–699
16. Agrawal S, Temsamani J, Tang JY: Pharmacokinetics, biodistribution, and stability of oligodeoxynucleoside phosphorothioates in mice. Proc Natl Acad Sci USA 1991, 7595–7599
17. Goodarzi G, Watabe M, Watabe K: Organ distribution and stability of phosphorothioated oligodeoxyribonucleotides in mice. Biopharm Drug Disp 1992, 13: 221–227
18. Plenat F, Klein-Monhoven N, Marie B, Vignaud JM, Duprez A: Cell and tissue distribution of synthetic oligonucleotides in healthy and tumor-bearing nude mice: an autoradiographic, immunohistological, and direct fluorescence microscopy study. Am J Pathol 1995, 147:124–135
19. Hoke GD, Draper K, Freier M, Gonzalez C, Driver VB, Zounes MC, Ecker DJ: Effects of phosphorothioate capping on antisense oligonucleotide stability, hybridization, and antiviral efficiency *versus* herpes simplex virus infection. Nucleic Acids Res 1991, 19:5743–5748
20. Fisher TL, Terhorst T, Cao X, Wagner RW: Intracellular disposition and metabolism of fluorescently-labeled unmodified and modified oligonucleotides microinjected into mammalian cells. Nucleic Acids Res 1993, 21:3857–3865
21. Crooke R: *In vitro* toxicology and pharmacokinetics of antisense oligonucleotides. Anticancer Drug Res 1991, 6:609–646
22. Bergan R, Connell Y, Fahmy B, Neckers L: Electroporation enhances c-*myc* antisense oligodeoxynucleotide efficacy. Nucleic Acids Res 1993, 21:3567–3573